Volume 60 Number 35 2 May 2024 Pages 4623-4734

ChemComm

Chemical Communications

rsc.li/chemcomm



ISSN 1359-7345



COMMUNICATION

Yun-Bao Jiang *et al.* Supramolecular helix of an oligomeric azapeptide building block containing four β -turn structures



ChemComm



COMMUNICATION

View Article Online



Cite this: Chem. Commun., 2024. 60, 4648

Received 30th September 2023, Accepted 11th March 2024

DOI: 10.1039/d3cc04859d

rsc.li/chemcomm

Supramolecular helix of an oligomeric azapeptide building block containing four β-turn structures†

Oligomers of benzoylalanine-based amidothioureas containing four β-turn structures spaced by meta-substituted benzenes were shown to undergo assembly in dilute CH3CN solution into supramolecular helices of enhanced supramolecular helicity, whereas those spaced by para-substituted benzene spacer(s) or those spaced by meta-substituted benzenes but with one or two β -turns exhibit a substantially decreased tendency of assembling.

Helical structures such as the protein α -helix and DNA double helix are of great significance in life sciences. Scientists have thus been exploring the design and development of diverse biomimetic artificial helices of varying functionalities. Supramolecular helical structures have attracted considerable attention also because of their adaptable cavity size, processability, flexibility, and ease of modification and functionalization. One strategy for constructing supramolecular helices is to elongate short building blocks in a helically folded conformation, through end-to-end noncovalent interactions. 1-4 Among them, aromatic foldamers of good predictability have been widely employed.⁵⁻⁹ Those helices can be applied to the recognition, encapsulation and transport of a variety of ions and neutral molecules, 6,10-12 and the properties of the supramolecular helices can be altered by structural adjustments thus to achieve regulated selectivity and activity. 13,14

Yet, the design of novel building blocks remains challenging. We have recently built single- and double-stranded supramolecular helices in the solid phase and in dilute solution, using a bis(N-amidothiourea) motif that contains two β -turns in the terminal or central parts of the molecule as the building block, such that the intermolecular halogen bonding bridges

^a Department of Chemistry, College of Chemistry and Chemical Engineering,

the MOE Key Laboratory of Spectrochemical Analysis and Instrumentation,

molecules into helices. 15,16 With these short building blocks, their concentrations might need to be high to allow a long enough helix to be well characterized, which may become hard as their solubility could be a limiting factor. The minimal optimal number of turn structures and the way of their linkage shall then be critical for their successful assembly into supramolecular helices.

Reported herein are our efforts to achieve amidothioureabased oligomeric building blocks that contain four $\beta\text{-turn}$ structures spaced by *meta*-substituted benzenes, 1L and 1D, taking, respectively, L- and D-alanine as the chiral source (Fig. 1a and b). Two iodine atoms are introduced at the parapositions of the two terminal phenyl rings to possibly afford intermolecular halogen bonding. Experiments show that these two oligomeric compounds function to assemble into stable supramolecular helices in dilute CH3CN solution, via halogen bonding. The para-substituted benzene-spaced counterparts do not assemble well (one of the four being para-substituted) or do not assemble at all (more than one) (3L, 4L and 5L, Fig. 1b), and those meta-substituted but containing one or two β-turns (6L and 7L, Fig. 1b) do not assemble either.

The β-turn structure in N-amidothiourea derivatives provides helical fragments. ¹H NMR spectra show that with increasing solution temperature, the chemical shift of each -NH proton in 1L moves downfield, at different rates (Fig. S1, ESI†). Notably, the resonance of the -NH^d proton exhibits the smallest temperature coefficient ($\Delta\delta/\Delta T = -2.44$ ppb °C *versus* $-NH^a$: -8.96, $-NH^b$: -8.73 and $-NH^c$: -8.76, Fig. 2a), indicating that it is less influenced by solution temperature. This means that it is protected, to some extent, agreeing with its taking part in an intramolecular hydrogen bond. Furthermore, the chemical shift of -NH^d remains unchanged upon changing the volume ratio of DMSO- d_6 to CD₃CN in their binary mixtures (Fig. S2 and S3, ESI†), providing further evidence for the presence of the hydrogen bonded β-turn.

Repetition of the β-turn structure, due to its helical character, may facilitate the elongation of the oligomeric building block. This will result in a folding propensity of the formed

Xiamen University, Xiamen 361005, China. E-mail: ybjiang@xmu.edu.cn ^b Fujian Provincial Key Laboratory of Innovative Drug Target Research and State Key Laboratory of Cellular Stress Biology, School of Pharmaceutical Sciences, Xiamen University, Xiamen, Fujian 361102, China

[†] Electronic supplementary information (ESI) available. See DOI: https://doi.org/

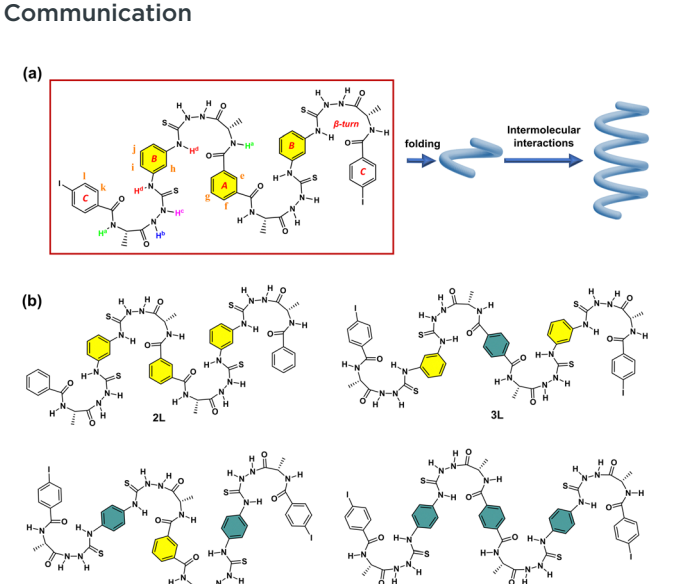


Fig. 1 (a) Chemical structure of 1L with numbering of protons and schematic illustration of the formation of a supramolecular helix from the helical oligomer. (b) Chemical structures of control compounds 2L, 3L, 4L, 5L, 6L, 7L and 1D

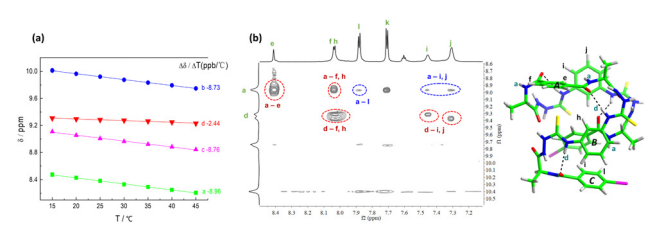


Fig. 2 (a) Influence of solution temperature on the resonance of the -NH protons of 1L in 90:10 (v/v) CD₃CN/DMSO-d₆ mixture and the fitted temperature coefficients. (b) Expanded 2D NOESY spectrum of 1L in DMSO- d_6 and DFT (M06-2X-D3/6-31G**)-optimized structure of **1L** in the gas phase. Dashed black lines highlight the intramolecular hydrogen bonds for the B-turns.

oligomer, indicated by the DFT-optimized structure of 1L in the gas phase (Fig. 2b). The 2D NOESY spectrum of 1L in DMSO- d_6 also reveals the folded conformation of 1L (Fig. 2b and Fig. S4, ESI†). NOE coupling signals between H^a-H^e and H^a-H^f indicate that the β-turns on two sides of benzene ring **A** are oriented in opposite directions. Similarly, the β-turns on two sides of benzene ring B also exhibit different orientations, as evidenced by the NOE signals between H^d-H^h, H^d-Hⁱ, and H^d-H^j. Furthermore, the NOE couplings between H^a-Hⁱ/H^j and H^a-H^l further proved that 1L is folded, which brings NH^a and benzene rings B and C into close proximity, in line with the calculated monomeric structure of 1L.

1L in the folded conformation may facilitate its supramolecular assembly, as a basic building block. We did observe such

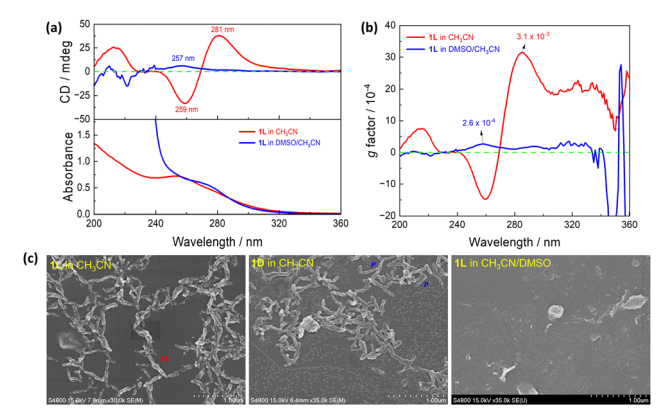


Fig. 3 (a) Absorption and CD spectra and (b) g-factor profiles of 1L in CH₃CN and in 1:199 (v/v) DMSO/CH₃CN. Due to weak absorbance in the range of 320-360 nm, the g-factor profiles within this region exhibit significant fluctuations. (c) SEM images of air-dried samples of 1L and 1D in CH₃CN and **1L** in 1:199 (v/v) DMSO/CH₃CN on platinum-coated silicon wafers. $[1L] = [1D] = 10 \mu M$.

supramolecular assembly in CH₃CN. In DMSO, a highly polar aprotic solvent, assembly of it would thus be much less, if any. Experiments in both pure CH₃CN and DMSO/CH₃CN binary solvents were carried out in detail. In CH₃CN, the absorption spectrum of 1L displays a band at 255 nm and a shoulder at 275 nm, accompanied by prominent Cotton effects at 281 nm, 259 nm, and 213 nm in the CD spectrum; in CH₃CN containing 0.5% DMSO by volume, however, only a faint CD signal at 257 nm was observed (Fig. 3a). Furthermore, the anisotropic factor, g, in CH₃CN (3.1×10^{-3} , Fig. 3b) is significantly higher, ca. 12 times that in DMSO/CH₃CN (2.6 \times 10⁻⁴, Fig. 3b). Dynamic light scattering (DLS, Fig. S5, ESI†) allows access to the size distributions of 1L in different solvents. The diameter of the 1L at the same concentration in DMSO/CH3CN was measured as 3.2 nm, whereas in CH₃CN it reached 22.8 nm. This further substantiates the assumption that 1L forms assemblies in CH₃CN, whereas in DMSO/CH₃CN it remains as a monomer. Meanwhile, SEM images of air-dried samples from CH₃CN solutions of 1L reveal the presence of ordered short M-helical assemblies and those of 1D the P-helical structures, whereas no regular morphology is observed from the samples prepared in DMSO/CH₃CN (Fig. 3c). These findings provide compelling evidence that 1L and 1D assemble into supramolecular helices in CH₃CN.

Supramolecular assembly occurs when the dimensionless concentration exceeds unity $(c_T K_e > 1)$, where c_T represents the total concentration and Ke refers to the equilibrium constant. Hence, a critical concentration, corresponding to K_e^{-1} , is required for the helical assembly of 1L to occur. 17 Indeed, CD signals of 1L in CH3CN measured at different concentrations indicate a remarkably low critical assembly concentration, ca. 1 µM (Fig. S6, ESI†), through which a high K_e value of $1.0 \times 10^6 \,\mathrm{M}^{-1}$ is estimated. Investigation into the concentration-dependent g factor of 1L reveals an increase in g with increasing concentration from 1 to 5 µM (Fig. S7, ESI†) after which it levels off. However, at a concentration below 1 μ M, the g factor varies

ChemComm

irregularly. Based on these observations, it is inferred that 1L exhibits a state of assembly instability at concentrations close to or below the critical assembly concentration, that the monomer and aggregates may exchange rapidly. As the concentration increases beyond this critical concentration, the monomer molecules assemble to lead to helical chain extension, indicated by an increase in the g factor. As the concentration approaches 5 μ M, the chain ceases to propagate, such that a stable assembly state is reached, which the g factor does not change any more. The concentration-dependent DLS data of 1L in CH₃CN corroborate this pattern of variation in g factor (Fig. S8 ν s. S7, ESI†). Consequently, it is concluded that the supramolecular helix of 1L in CH₃CN possesses a finite size range, rather than an infinite extension.

According to our previous research, 15,16 it is assumed that the supramolecular helix of 1L is probably driven by intermolecular halogen bonding. Thus, control compound 2L (Fig. 1b), without I-substituents, was examined. First, in CH₃CN the CD intensity of 2L is significantly weaker than that of 1L, with no discernible CD signal associated with the assembly (Fig. S9, ESI†). Second, upon increasing the concentration of 2L, no obvious changes were observed (Fig. S10, ESI†). Third, the g factor of 2L reaches a maximum value of 3.1×10^{-4} at 244 nm (Fig. 4a and Fig. S11, ESI†), one tenth that of the maximum value of 1L (3.1×10^{-3} at 285 nm). It is reasonable to conclude that 2L is unable to assemble into supramolecular species in CH₃CN. Indeed, DLS experiments reveal that the diameters of 2L in CH₃CN are around 3.3 nm (Fig. S12, ESI†), approximately 7 times smaller than those of 1L. No assembly morphology was observed in the SEM images of 2L (Fig. S13, ESI†). Taken together, it is concluded that control compound 2L does not undergo assembly in CH₃CN, suggesting thus the role of I-substituents in 1L in driving its assembly into supramolecular helices.

Halogen bonding was further supported by examining in solvents of different alkalinity. On addition of a 20% volume fraction of H₂O into CH₃CN, the CD spectrum of **1L** experiences a significant change and a weakening of the intensity. In contrast, addition of 20% by volume THF, a solvent of weaker electron donating capacity, results in a minor change in the CD spectrum. These observations support the hypothesis that halogen bonding serves as an interaction force between

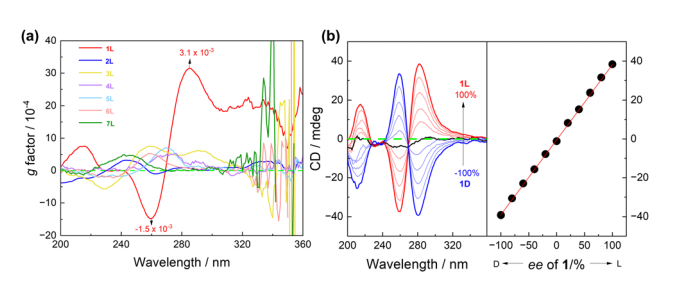


Fig. 4 (a) Wavelength profiles of the g factors of 1L-7L in CH $_3$ CN. $[1L-5L] = 10 \mu$ M, $[6L] = 40 \mu$ M, and $[7L] = 20 \mu$ M. (b) CD spectra of mixtures of 1L and 1D of various ee in CH $_3$ CN and plots of the CD signals at 281 nm against ee. $[1L] + [1D] = 10 \mu$ M.

molecules (Fig. S14–S16, ESI \dagger). ¹⁸ Cl $^-$, Br $^-$, and I $^-$ anions can act as halogen bond receptors, and their ability to destroy halogen bonds follows the order of I $^-$ > Br $^-$ > Cl $^-$. ¹⁹ On addition of halogen anions at a high concentration of 100 equivalents into CH₃CN solution of 1L, the CD signal of the supramolecular species of 1L gradually decreases (Fig. S17, ESI \dagger), and the order of intensity decline is the same as their destructive ability towards halogen bonds, *i.e.*, I $^-$ > Br $^-$ > Cl $^-$ (Fig. S18, ESI \dagger).

NMR spectra also support the existence of intermolecular halogen bonding. In comparison to the ¹H NMR spectrum of monomeric 1L in pure DMSO- d_6 , we observed additional weak ¹H NMR signals of **1L** in CD₃CN/DMSO- d_6 (200:1, v/v) (Fig. S19, ESI†), which were assigned to the assembled oligomers, as evidenced by the COSY couplings of Hk'-Hl', Hf-Hg' and H^{f'}-H^{g'} (Fig. S20, ESI†). Interestingly, clear NOESY coupling signals are shown for H^e-H^k, H^e-H^l, H^f-H^k, H^f-H^l and H^j-H^l in $CD_3CN/DMSO-d_6$ (200:1, v/v), but no such couplings are observed in DMSO- d_6 at the same concentration. According to the calculated structure of monomeric 1L, pairs of protons H^e-H^k, H^e-H^l, H^f-H^k, and H^f-H^l are too far apart to be intramolecularly coupled. Only when the intermolecular C-I...O bonds link adjacent 1L molecules, benzene ring C in which H^k and H^l are located will be brought into close proximity to benzene ring A from another 1L molecule that contains H^e and H^f, resulting in clear intermolecular coupling signals (Fig. S21, ESI†). We thus proposed that the formation of supramolecular assemblies of 1L is driven by intermolecular C-I···O halogen bonding.

In 1L, the β -turn provides the helical conformation, four of which are spaced by *meta*-substituted benzene rings, which is more conducive to the propagation of the helicity of the turn structure. We thus developed control compounds 3L, 4L and 5L, containing, respectively, 1, 2, and 3 para-substituted benzene spacers (Fig. 1b). CD spectra in CH₃CN show that these three control compounds exhibit weaker CD intensities than 1, and the signal peaks appear at shorter wavelengths (Fig. S22, ESI†). The g factor values of 3L, 4L, and 5L are significantly smaller than that of 1L (Fig. 4a). This finding further supports the superior propagation of the helicity of 1L and highlights the synergy of the meta-substitution at the benzene spacers in facilitating the transmission of homochirality. In addition, we compared the spectra of the control compounds containing different numbers of β-turns, 6L containing only one and 7L containing two (Fig. 1b). The CD spectra show that at the same concentration of the β-turn in 1L, 6L, and 7L, 1L in CH₃CN exhibits a much higher CD intensity and a larger g factor than those of 6L and 7L (Fig. 4a and Fig. S23, ESI†). Even at increased concentrations of 60 µM for 6L and 200 µM for 7L, no assembly was observed (Fig. S24 and S25, ESI†). This suggests that the size of the oligomeric building block is important too, and smaller does not guarantee a stronger tendency of assembly, despite being less flexible. In view of the SEM images, none of the control compounds (2L, 3L, 4L, 5L, 6L and 7L) were found to assemble into helical aggregates in CH₃CN (Fig. S26, ESI†). It is of interest to recall that the para-substituted benzene spaced

Communication ChemComm

counterpart of 7L containing two β-turns undergoes assembly into helices in dilute CH₃CN, ¹⁵ again highlighting the critical role of the spacer that links the β -turn structures.

Temperature-dependent CD signals of 1L in CH3CN show that the helix is highly heat stable. The CD intensity was only slightly reduced upon heating the solution up to 70 °C and it can be completely restored after cooling (Fig. S27 and S28, ESI†). The enantiomeric mixtures of 1L and 1D of varying ratios in CH₃CN show a linear-dependence of the CD signals on the enantiomeric excess (ee) (Fig. 4b), suggesting that the enantiomers of 1L and 1D are self-sorting in their assemblies. 20,21 This is different from the single-stranded helix from the building blocks via $C-I \cdots \pi$ halogen bonding (S-shaped CD-ee dependence), 15 but similar to that of the double helix driven by two crossed C-I···S halogen bonds. 16

In summary, an oligomeric building block that contains four β-turns using a benzoylalanine-based amidothiourea motif is shown to be of optimal minimum length to allow efficient assembly into a supramolecular helix. 1L or 1D in which four β-turn structures are spaced by *meta*-substituted benzene rings undergoes assembly in CH₃CN at a µM-level concentration, via intermolecular halogen bonding. The formed helix exhibits strong CD signals of a high g factor of 3.1×10^{-3} at 285 nm for instance and a linear CD-ee dependence, together with an excellent thermal stability. DLS data show that the length of the formed supramolecular helix is finite. Replacing the metasubstituted benzene spacers with para-substituted one(s) substantially decreases the tendency of assembling, highlighting the critical role of helicity propagation in facilitating the helical assembly, and neither does a decrease in the number of β -turns spaced by *meta*-substituted benzenes. We therefore show that with oligomeric helical building blocks, an optimal number of turns and the way they are spaced are important factors dictating their assembly into helices.

This work has been supported by the National Science Foundation of China (Grants 21820102006, 22101240, 22241 503 and 92356308), the Fundamental Research Funds for the Central Universities (Grants 20720220005 and 20720220121), and the Natural Science Foundation of Fujian Province of China (No. 2023J01038).

Conflicts of interest

The authors declare no conflicts of interest.

Notes and references

- 1 C. Z. Liu, M. Yan, H. Wang, D. W. Zhang and Z. T. Li, ACS Omega, 2018, 3, 5165-5176.
- 2 E. Yashima, N. Ousaka, D. Taura, K. Shimomura, T. Ikai and K. Maeda, Chem. Rev., 2016, 116, 13752-13990.
- 3 M. Gonzalez-Sanchez, M. J. Mayoral, V. Vazquez-Gonzalez, M. Paloncyova, I. Sancho-Casado, F. Aparicio, A. de Juan, G. Longhi, P. Norman, M. Linares and D. Gonzalez-Rodriguez, J. Am. Chem. Soc., 2023, 145, 17805-17818.
- 4 Q. Gan, Y. Wang and H. Jiang, Chin. J. Chem., 2013, 31, 651-656.
- 5 D. J. Hill, M. J. Mio, R. B. Prince, T. S. Hughes and J. S. Moore, Chem. Rev., 2001, 101, 3893-4012.
- 6 H. Juwarker, J. M. Suk and K. S. Jeong, Chem. Soc. Rev., 2009, 38, 3316-3325
- 7 D. W. Zhang, X. Zhao, J. L. Hou and Z. T. Li, Chem. Rev., 2012, 112, 5271-5316.
- 8 D. W. Zhang, W. K. Wang and Z. T. Li, Chem. Rec., 2015, 15, 233-251.
- 9 C. Z. Liu, S. Koppireddi, H. Wang, D. W. Zhang and Z. T. Li, Angew. Chem., Int. Ed., 2019, 58, 226-230.
- 10 T. Yan, F. Yang, S. Qi, X. Fan, S. Liu, N. Ma, Q. Luo, Z. Dong and J. Liu, Chem. Commun., 2019, 55, 2509-2512.
- 11 Y. Ferrand and I. Huc, Acc. Chem. Res., 2018, 51, 970-977.
- 12 C. Zhang, X. Deng, C. Wang, C. Bao, B. Yang, H. Zhang, S. Qi and Z. Dong, Chem. Sci., 2019, 10, 8648-8653.
- 13 X. Yan, P. Weng, D. Shi and Y.-B. Jiang, Chem. Commun., 2021, 57, 12562-12574.
- 14 D. Bindl, P. K. Mandal and I. Huc, Chem. Eur. J., 2022, 28, e202200538.
- 15 J. Cao, X. Yan, W. He, X. Li, Z. Li, Y. Mo, M. Liu and Y.-B. Jiang, J. Am. Chem. Soc., 2017, 139, 6605-6610.
- 16 X. Yan, K. Zou, J. Cao, X. Li, Z. Zhao, Z. Li, A. Wu, W. Liang, Y. Mo and Y.-B. Jiang, Nat. Commun., 2019, 10, 3610.
- 17 M. M. Smulders, M. M. Nieuwenhuizen, T. F. de Greef, P. van der Schoot, A. P. Schenning and E. W. Meijer, Chem. - Eur. J., 2010, 16,
- 18 C. Laurence, M. Queignec-Cabanetos, T. Dziembowska, R. Queignec and B. Wojtkowiak, J. Am. Chem. Soc., 2002, 103, 2567-2573.
- 19 A. Mele, P. Metrangolo, H. Neukirch, T. Pilati and G. Resnati, J. Am. Chem. Soc., 2005, 127, 14972-14973.
- 20 X. Yan, Q. Wang, X. Chen and Y.-B. Jiang, Adv. Mater., 2020, 32, e1905667.
- 21 C. Roche, H. J. Sun, M. E. Prendergast, P. Leowanawat, B. E. Partridge, P. A. Heiney, F. Araoka, R. Graf, H. W. Spiess, X. Zeng, G. Ungar and V. Percec, J. Am. Chem. Soc., 2014, 136, 7169-7185.